Technical Solutions in Dimensioning an Industrial Torrefaction Facility

Jonathan Bergman

Masters thesis, 30 ECTS, for the degree of Master of Science in Energy Engineering, Department of Applied Physics and Electronics, Umeå University, 2017

EN1608

Examensarbete för civilingenjörsprogrammet i Energiteknik, 30 hp

Umeå Universitet

Abstract

Torrefaction is a process where biomass is subjected to temperatures between 240-350°C, in an oxygen deficient environment, between 2 and 60 minutes. The purpose of torrefaction is to improve the properties of the biomass. After the process, the biomass has a number of advantages compared to untreaded biomass, such as higher energy density and better grindability.

During the summer of 2015, Bioendev AB started an industrial demonstration unit (IDU), located in Holmsund, with an output capacity (NPC) of 2000 kg_{DS}/h. During the design and construction of the IDU, the risk of dust explosion led to large cost increases. Therefore, the entire torrefaction reactor and connected equipment needed to be classified as a pressure vessel capable of withstanding 4.5 Bar_g. The plant also needed large check valves and bursting discs. The next torrefaction plant that Bioendev builds will need to be significantly bigger than the IDU, and thus the technical challenges due to the dust explosion problems will be even greater.

Therefore, BioEndev aims to evaluate solutions that avoid classification of the reactor as a pressure vessel, or to identify and solve problems regarding explosion venting for the current design during upscaling. This master thesis processes and investigates possible technical solutions for the physical problems that may arise when scaling-up the torrefaction plant.

The method was begun to identify the vital components of the torrefaction system and operational parameters, it was important to be able to determine flows and how these operate inside the system. Since the structure of the system was known, it was possible to begin the calculations of the energy and mass balances in the system. By determining the molar flow in the system the pipe dimensions could be determined.

The reactor was designed according to demands that were found in the standards for pressure vessels. It was also designed on the basis of a physical limitation found through tests on the reactor at the IDU, where the degree of filling was found to be the main limitation of the volume of biomass through the reactor.

To calculate the ventilation area needed to reduce the pressure of an explosion, NFPA 68: 2007 was followed.

Simulations of flows were made primarily to study the pressure drop across the components in the system. Even simulations with moving parts were performed, to study the shutter speed at higher pressure shocks.

The overall conclusion of this thesis is that there are numerous complexities in scaling-up a facility. For example, breaking strength scales according to cross-sectional area, while the stiffness of the materials scales according to length. In this thesis, the sizing was made by scaling the system geometrically, based on benchmark tests on the IDU. This only provides a hint of the right solution.

This means that new FEM analyses and calculations for each part need to be performed. The findings of this thesis indicate that it may be possible to upscale 3 to 6 times, according to IDU's capacity, without any major risks. In order to make a final decision about the size an industrial unit can be scaled to, in accordance to the IDU, the conveyor screw needs to be investigated. Bioendev needs to know the size that is possible, based on self-weight ratio, heat and design.

One of the technical challenges was to investigate the check valve and what problems a bigger system might be exposed to, and how that will affect the function of the check valve. In my study, there was no sign that the check valve, nor the BPS (baffle for pressure surge), will be a problem.

There was also an investigation of whether the reactor should be designed for a lower pressure. The results showed that there was not enough external space around the reactor for the required amount of bursting discs.

This thesis enables continued study of the structural challenges and provides answers to Bioendev about whether the conveyor screw, or other components, can be manufactured in accordance to standards and safety regulations.

Acknowledgement

This thesis comprises 30hp. It is a Master's thesis submitted in the Master Programme in Energy Technology, at Umeå University. The work was carried out on behalf of Bioendev AB.

To begin with, I wish to thank my supervisor from Bioendev, Ingemar Lindh, who helped with all relevant data around the plant. He has also been instrumental in matters large and small.

I also wish to thank my supervisor from the Department of Applied Physics and Electronics, at Umeå University, Markus Broström.

Finally, I would like to thank Richard Langlais who helped me to review the language in this thesis.

Table of Contents

1. Introduction

Humanity's current dependence on fossil fuels is not sustainable, neither from a climate perspective, nor from the fact that there is only a limited amount of raw material. Many countries have begun to realize that this dependence must decrease. This was demonstrated during the COP 21 meeting, in Paris [1]. With an increased share of renewable energy in the community, even higher demands will be placed on its efficiency and reliability. This is both an opportunity and a challenge for the future [2]. Therefore, the use of biomass for production of heat and electricity is timely, especially since the EU target for 2020 is that 20% of the input energy shall originate from renewable sources [3]. There is also great interest in burning 100% pulverized biomass in converted coal-fired power plants, as the plant owners may be forced to stop burning fossil coal under the EU Large Combustion Plant Directive [4]. Moreover, after 31 March 2016, the co-firing plants that are not able to meet current flue gas, sulfur and NOx removal levels will not be granted the Renewable Obligation Certificate, while the plants that are fired by 100% renewable fuels will [5].

Combustion technology is currently the most common technology in Sweden for heating buildings, from houses up to Central Heating Plants (CHP), with biofuels. In order to produce renewable energy, there are requirements that the fuels need to meet, so that the combustion plant avoidsbeing damaged [6]. The combustion of solid materials creates particle emissions.

To improve the combustion of solid materials, research is studying how to refine the old technology that has been practiced for many thousands of years; in modern times, it has been used in so-called charcoal stacks, which until the 1950s accounted for the main supply of charcoal burned in Swedish blast furnaces [7].

The process in which organic material is heated in an environment with limited oxygen supply is called pyrolysis [8]. Pyrolysis is a thermo-chemical process [9], where cellulose and lignin degrade from long to short carbon chains [10]. In the process of pyrolysis, coal and gas are formed. Pyrolysis gas contains primarily bio oil and synthesis gas, which in turn contain long hydrocarbon chains and methane, hydrogen, carbon monoxide and carbon dioxide. The solid product is called coal and is used as an energy carrier. The uses of biochar are as soil conditioners, animal feed supplements, filter materials for water treatment and carbon storage [11]. Biochar is defined as coal that is produced by pyrolysis, for use in agriculture (and other non-thermal uses), in an environmentally sound and sustainable manner. To fulfill biochar certification, there are also requirements for biomass used as fuel [12]. The pyrolysis gas can be used to produce heat in a burner [9].

The pyrolysis process requires less supplied fuel than traditional combustion. Since it is a gas that is burned, it avoids the problems related to combustion of solid fuel: emissions of chlorine, alkalis, particles and sintering [9]. This means that it is possible to use fuels that are more difficult to burn, which today can be a problem. One of these fuels is horse manure, which has become a burden for many horse owners, because it requires a large spreading area and is not given away to area farmers in an unregulated manner, which is when contamination may occur. Also, biomass with lower energy content, such as poor-quality straw, or reeds, currently have few uses, but can be pyrolyzed.

The coal produced in the pyrolysis process has many potential uses, including as a soil improver. There are comprehensive studies of the effects on arable productivity of spreading coal that is loaded with nutrients and spread on cropland. An additional effect is that the carbon will be locked in the ground and have the same function as carbon storage [11]. Another technology in the pyrolysis area is torrefaction.

Torrefaction is increasingly becoming understood to be an interesting thermochemical method for improving biomass as an energy carrier, for 100% replacement of fossil coal. The method improves the qualities of the biomass and makes it more coal-like; this includes such qualities as increased heating value, increased energy density, increased material friability, improved resistance to biological decay

and being less hydrophilic (less water uptake) [13]. Torrefied biomass is also known by such names as biochar, green coal, charcoal, or biocoal. However, these names can easily be confused with the solid product from the pyrolysis processes, and should be avoided. The temperature of the biomass during the torrefaction process usually varies between 240 °C and 350 °C; the residence time varies from 2 minutes up to several hours [13].

To produce torrefied biomass, the standard process is to encapsulate the biomass in an environment where the pressure is ambient and the atmosphere is inert, to avoid oxidation and prevent the biomass from catching fire. At the IDU, the torrefied biomass is produced by letting the biomass feed through the torrefaction reactor using a screw conveyor. This allows the fine fragments that arise during transport through the reactor to mix with the torrefaction atmosphere that prevails inside the vessel. Under these circumstances, it is possible for a dust explosion to occur, if the control of the low oxygen content fails. In order to prevent injuries or fatalities, a good understanding of dust explosions and the measures that will reduce the frequency and impact of such an event must be gained.

The process must begin with the supply of external energy; today, LPG or electricity are often used [12]. Once the process has been started, there is no need to add more energy, because the exothermic reaction will have begun. This means that the process produces heat and will continue for as long as new fuel is added [9].

The first thing that occurs in the reactor is that water starts to evaporate from the biomass, that is, fibrous biomass, containing mainly cellulose, hemicellulose and lignin [11], but also a certain amount of extractives [9]. Extractives are, in particular, cellulose pulp and consist of compounds that are soluble in petroleum ether, diethyl ether, dichloromethane, acetone, ethanol and water [14]. Lipids, terpenoids, phenols, glycosides, small carbohydrates, pectin, starch and protein compounds belong to extractives [14]. The composition of the cellulose, hemicellulose and lignin varies according to different types of biomass. Variations also occur in the same type of biomass when ithas grown in different soils, in different climatic zones and harvested at different times Cellulose, hemicellulose and lignin all behave differently at different heating rates and temperatures. Hemicellulose is the first to decompose, between 220 and 315° C. The cellulose starts its degradation at 315° C. and continues to 400° C. Lignin has a slow, but stable, degradation process, which begins at 160° C and continues to 900° C [11]. The minerals are generally left in the carbon, but are then called ash [9].

A company called Bioendev has realized the benefits of torrefaction; it is also the company that I have had the privilege of doing my thesis for. Bioendev is an innovative technology development company founded by Professor Anders Nordin and Ingemar Lindh, in 2007. Their mission is to develop and supply high-tech systems that enable the most efficient refining of biomass for use in CHP systems, in conversion to fuels and the production of green chemicals. As a first step in achieving this, Bioendev has developed a cost-efficient technology for producing torrefied and densified biomass. Bioendev's solution has superior process control and high utilization, and produces a product with very high quality.

Today, Bioendev operates a pilot plant and has an Industrial Demonstration Unit.

Together with its Engineering, Procurement and Construction (EPC) partner, Bioendev will be selling turnkey torrefaction plants ranging from 100-200 kton production per year. Bioendev also offers retrofitting of white pellet plants to torrefaction [15].

1.1 Dust explosions inside closed vessels

In the torrefaction system, fines will occur as the biomass is transported through the system. If the fines are in the atmosphere inside the system they will be defined as a dust cloud. A dust cloud can be seen as a gas mixture. To ignite it, the following criteria must be met: 1) combustible particulates sufficiently small to burn rapidly, 2) a source of ignition, 3) a suspended cloud of particulates at a concentration above the Minimum Explosible Concentration (MEC), 4) confinement of the dust cloud by an enclosure and 5) sufficient oxygen, greater than the Limiting Oxygen Concentration (LOC) [16].

Real-world testing shows that the Theoretical Flame Temperature (TFT), i.e., the adiabatic flame temperature of the burning dust cloud, needs to reach at least 1500K for a dust explosion to occur. Calculations show that this corresponds to approximately 12% for torrefied dust.
When the gas cloud is ignited, there are two modes that can occur. These modes are deflagration and detonation. Deflagration is the most common type of flame propagation. It propagates at subsonic speed relative to the unburned gas. The flame speed seen by an observer is between 1 to 1000 m/s and the pressure builds due to the speed it achieves. Detonation is a supersonic combustion wave, where the combustion wave and the shock wave are, in this case, coupled. The detonation wave will propagate at a velocity of 1500-2000 m/s and the peak pressure varies between 15 - 20 bar_g [16]. In order to design the parts of the IDU, Bioendev AB hired DEKRA to analyze the maximum explosion pressure (P_{max}) and the deflagration index (K_{st}) in an explosion vessel Kuhner 20L Sphere. In a literature review undertaken for this thesis, it was found that it is difficult to manage biomass powder in such a small container. Due to the low bulk density of biomass, the dust holder is actually too small to contain the amounts needed for characterization, and it is therefore necessary to use a bigger vessel and dust holder. The K_{st} and P_{max} values are often over- or underestimated [17]. When an internal explosion in a pressure vessel is analyzed, the most important parameter in determining the pressure build-up is the size of the gas cloud. The maximum pressure in a closed container will appear when the combustion is completed. For most hydrocarbon fuels, stoichiometric combustion of the fuel and air cloud will create a pressure between 7-10 bar at 1ATM [18].
Besides the closed vessel, i.e., the torrefaction reactor, the plant also contains pipes. In pipes, there is a possibility that the flame propagates away from the combustion front, and that high speeds generate a high explosion pressure. The main mechanism that allows the flame to accelerate in the pipe is turbulence. When the gas burns, it expands and pushes the unburned fuel ahead of the flame front. This flow of unburnt fuel creates a turbulent boundary layer and will enhance the burning rate [16].
To protect the torrefaction system and the people who work with it, safety components need to be installed in the torrefaction reactor according to some applicable standard. In Bioendev's case, NFPA 68: 2007 was used. The design of the reactor has to account for the worst-case scenario. At the IDU, this scenario has been assumed to be a dust explosion. If the reactor were built to withstand the pressure of such an explosion, the shell would have a thickness in accordance to EN 13445-3 7.4.2. This would lead to a higher manufacturing cost, in terms of manufacture and materials. This is a known problem in the industry, and can be solved by installing connections to the shell that will burst, and hence lead the explosion pressure away to a safe area. These thinner parts can be bursting discs or bursting panels. Bioendev followed NFPA and was subsequently approved by the third-party auditor, Inspecta.

1.2 Objective

The aim of this thesis is to assist Bioendev in anticipating problems that may emerge from a new design for a commercial plant.
To begin scaling the system, it will first be necessary to investigate it and understand its workings. The system can therefore be designed to an appropriate size for a specific Name Plate Capacity (NPC), which is the maximum capacity. Once this is done, the understanding of the system will have increased, and suggestions for possible solutions to the challenges can be presented and, hopefully, investigated. The objectives of the present work are therefore to 1) perform an energy and mass balance of the proposed torrefaction system. This will enable the identification of all the flows and temperatures needed for sizing the system; 2) determine the maximum size of a similar IDU torrefaction reactor with regards to the pressure vessel, pressure relief devices, check valves, pipes and ducts; 3) determine the technical challenges of such a system; and 4) possibly solve or propose solutions to some of the technical challenges.

To start with the design study, the earlier literature study and data from Bioendev was used. The time for producing this thesis was limited, and it was therefore not possible to answer questions that may arise in the construction work that will be the next step after the design study. No major financial analysis has been conducted, since this was beyond the scope of the work.

2 Design considerations

The reactor is the heart of the pyrolysis process where the reaction occurs, and where the biomass pyrolyzes to pyrolysis gas and coal. The reactor needs to withstand high temperatures, up to 500 °C in this case. The temperature must not fluctuate more than 20% of the planned reactor temperature, since it may have effects on the quality of the product.

One of the reactor's primary functions is to secure a low oxygen <2%. [12]. If the fuel has a low energy density it is easy to burn it up instead of its being pyrolysed. Bioendev has solved this by alternating the residence time in the reactor, and thus decreasing the risk of fuel burning up instead of being charred. In Figure 1 the torrefaction system is presented.

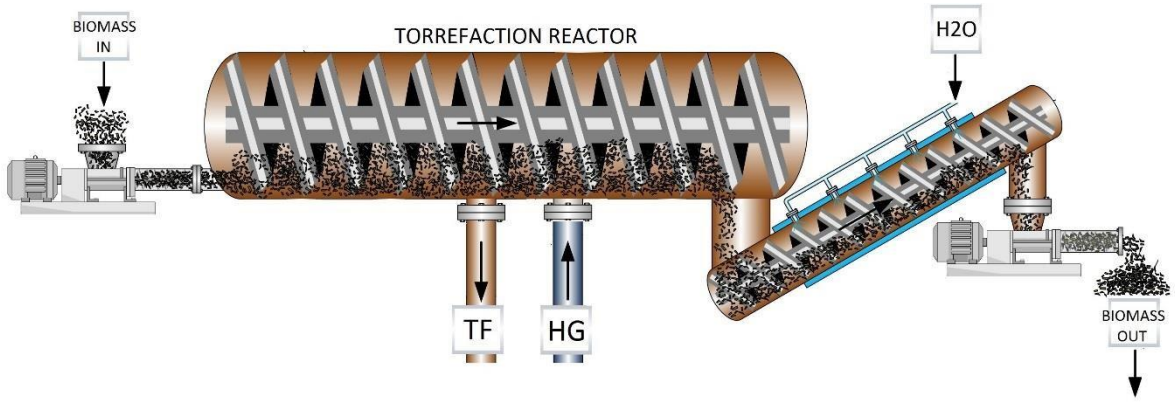

Figure 1 The biomass flow through the torrefaction reactor; TF is the torrefaction gas leaving the process as fuel to the burner, HG is the hot gas recycling from the combustor

Through a benchmark test, Bioendev found that the degree of filling of the reactor could not exceed a certain level. When that occurred, biomass then began to climb over the center shaft and then fall over to the previous screw turns, and thus commenced transport of a portion of the biomass in the opposite direction than what was intended. From the benchmark test, the following data could be obtained, as in Table 1.

Table 1 Displays the data that is relevant from the benchmark test.

Benchmark		
Biomass Density	112,6	$kg_{Ds}/\,m^3$
Rotation speed at 70 Hz, rpm_{70Hz}	1,72	rpm
Volume out, V_u	1,03	m^3
Time, T_m	108	s
Number of screw turns, a_S	16	pcs

To calculate the fill rate in the torrefaction reactor, the segment area has to be determined in accordance with

$$A_s = \frac{1}{2} {r_{R_i}}^2 (\theta - \sin\theta) \tag{1}$$

where r_{Ri} is the inner radius of the reactor and θ is the angle of the segment calculated by the following equation

$$\theta = 2arcsin\left(\frac{r_s}{r_{R_i}}\right) \tag{2}$$

where r_S is the segment radius and is determined by

$$r_s = \sqrt{h_s(r_{R_i} - h_s)} \tag{3}$$

h_S is the height of the segment, which is set to the screw blade height. The reactor internal cross-section area is then calculated as

$$A_{Ri} = \pi {r_{Ri}}^2 \tag{4}$$

and then one can calculate the fill rate as

$$F_{Rb} = \frac{A_s}{A_{Ri}} \tag{5}$$

As the conveyor screw in the reactor moves the biomass forward, the shape of the segment will have a more teardrop-shaped geometry. Thus, the calculated fill rate is slightly higher than the real one. The difference between calculated and real fill rate will be investigated during a real benchmark test. To calculate the fill rate by using the benchmark data in Table 1, the following formula is used to find the volume flow, $\dot{V}_f$.

$$\dot{V}_f = V_u \frac{3600}{t_m} \tag{6}$$

where V_u is the control volume out of the reactor and t_m is the time it takes to fill the control volume. The residence time is determined by

$$t_u = \frac{a_s}{rpm_{70_{Hz}}} \tag{7}$$

where a_S is the number of screw blades and $rpm_{70_{Hz}}$ is the rotational speed at 70 Hz. Then the total wood volume V_T in the reactor is calculated by using the following formula,

$$V_T = t_u \frac{V_f}{60} \tag{8}$$

and the empty volume of the reactor is then calculated based on the length of the chip bed,

$$V_{Ra} = V_T - V_{Rs} \tag{9}$$

where V_{RS} is the volume of the conveyor screw based on the chip bed. Then the fill ratio based on the Benchmark is calculated as

$$F_{Bm} = \frac{R_T}{V_{Ra}} \tag{10}$$

and then the volume flow is converted to mass flow by using

$$\dot{m}_f = \dot{V}_f \rho_f \tag{11}$$

where ρ_f is the density of the biomass with respect to dry substance.
In order to calculate the amount of biomass needed to feed the plant to meet the desired NPC, the following formula is used

$$\dot{m}_{fin} = \frac{NPC}{\mu_{74\%}} \tag{12}$$

where NPC is Name Plate Capacity and $\mu_{74\%}$ is in the gas exchange in the process. Then, the design maximum volume flow is determined with

$$\dot{V}_{dim} = \frac{\dot{m}_{fin}}{0{,}504\rho_f} \tag{13}$$

where 0.504 is the ratio between the nominal and maximum capacity at IDU.
Further, by using the lowest residence time, the maximum volume according to the chip bed can be determined by

$$V_{dim} = \dot{V}_{dim} t_u \tag{14}$$

and the new total reactor volume can now be calculated with the following formula

$$V_{Rdim} = \left(1 - \frac{l_{Rf}}{l_{RT}}\right)\frac{V_{dim}}{F_{Bm}} + \frac{V_{dim}}{F_{Bm}} \tag{15}$$

where l_{Rf} is the length of the biomass chip bed at the IDU and l_{RT} is the inner total length of the reactor at the IDU.
Then, the new total reactor volume is calculated by first determining a ratio between length and diameter in accordance with NFPA 68 2007. Thereafter, the total length of the reactor is calculated by the following formula

$$l_{dim} = \sqrt[3]{\frac{(2R_{dim})^2 V_{Rdim}}{\pi}} \tag{16}$$

where R_{dim} is the ratio determined by

$$R_{dim} = \frac{l_{dim}}{D_{dim}} \tag{17}$$

where D_{dim} is the new diameter of the reactor. We now know how long the reactor will be at this ratio and its diameter depending on the desired NPC.

2.1 Design of the hot gas tube reversal

When designing the size of the piping that is adding energy from the combustor to the reactor in the form of hot gas, the required energy of the torrefaction process and the pressure drop in the tube need to be considered.

2.1.1 Required Energy for the torrefaction process

By means of a literature review, previous research on the required energy demand was obtained [19]. Q_{rq} is the energy calculated as necessary to torrefy biomass to a specific mass yield, including moisture at a certain torrefaction temperature. The biomass input temperature is around 25°C. Because the state is not adiabatically in the system, a loss factor has to be added. The needed effect for a specific biomass flow into the facility can now be calculated.

2.1.2 Energy in cast pyrolysis

In order to calculate how much energy there is in the cast pyrolysis, the thermochemical data have been analyzed in the computer program, Factsage 5.2, to find a curve fitting. The curve fitting was used to find the enthalpy of the pyrolysis gas at a certain temperature.

The available effect in the first part of the combustion chamber could then be calculated by using heating value for the biomass [19]. The data shows the quantity of gas developed per kilogram of dry biomass and the composition of the gas. A combustion calculation could then begin.

By determining the moisture content of the biomass when it enters the torrefaction process from the drying system, it is possible to determine how many moles of water discharged from the biomass to the flue gases. As a result, the mass of the total fuel and the total oxygen demand per kg of dry biomass could be determined.

In order to go further and determine the total stoichiometric air requirements that will be needed in the burning process, we need to determine the raw nitrogen that enters, with the air, into the combustion, because it is not actively involved in the combustion. The molar amount of dry air that is crucial for the combustion can be calculated by adding the oxygen of the dry air to the molar amount of the raw nitrogen.

In addition to the air composition, in the air there is also moisture that does not bind molecularly. This moisture is assumed to be 1% of the dry air. With these assumptions and data, the stoichiometric air requirement for combustion can be calculated for each kg of dry substance biomass.

After the stoichiometric combustion gases are determined, we need to set an excess air. Lambda needs to be greater than 1; in this calculation lambda is determined to be 1.3. The dry air, the moisture and the dry flue gases can then be determined. This leads to a possible determination of mole flow of gases through the chimney and its composition based on the biomass flow into the reactor, noting that the molar mass in and out of the system is different. It will increase in the combustion. This can mostly be attributed to the combustion of the hydrogen from the fuel, and the fact that the fuel has to contain moisture to evaporate.

Even the steam generated in the cooling screw needs to be calculated. Since the mole flow in the chimney is determined, we know what is coming into and what is leaving the system. The energy and mass balance of the system can begin.

When we have found the various fractions of the flue gas compositions, we can use FactSage 5.2 and data from a database [20] to analyze the thermochemical properties for the different gas compositions. Based on the results from FactSage, and by using Hess's Law, a curve fitting could be constructed to find the enthalpy depending on the temperature.

2.1.3 Energy and mass balances in the system

The energy and mass balances require knowledge of the system buildup. In Figure 2, the torrefaction system is illustrated. Since the development of gas from the biomass, the composition and also the enthalpy depending on the temperature are known, it is possible to determine the energy balance of the whole system.

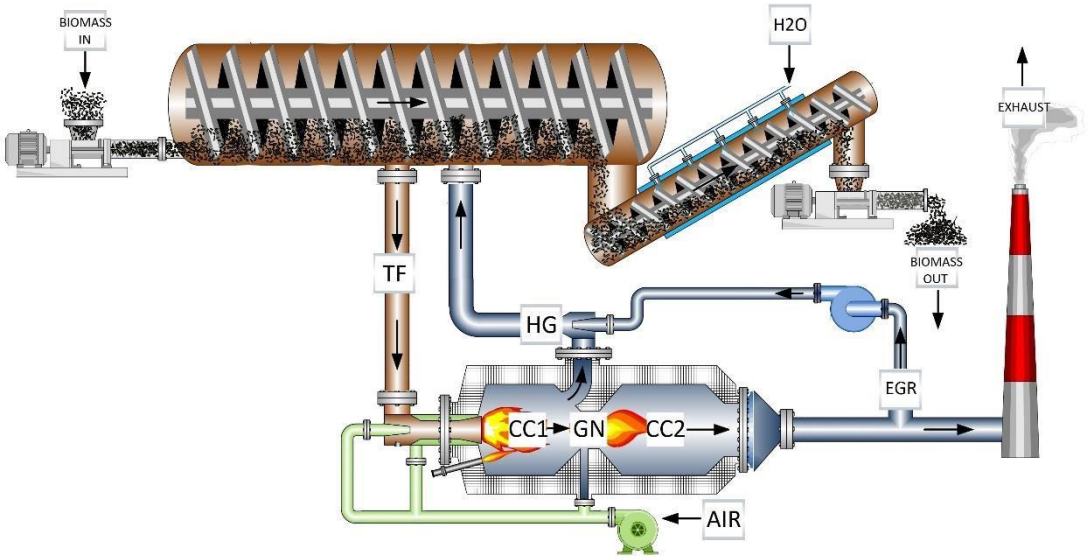

Figure 2 Simplified picture of the flow of gas in the system, the TF is torrefaction gas, HG is hot gas, CC1 is the combustion gas in the combustion chamber 1, GN is combustion gas in the gas neck, CC2 is combustion gas in the combustion chamber 2, EGR is the percentage of exhaust gas recirculation, H2O is cooling water which forms steam, AIR is the total air demand including excess air.

To simplify, we break down the system into two parts. One part is analysis of energy from biomass, and of water and hot gases. Another part is analysis of energy, from the torrefaction process to the burner. The energy and mass balance throughout the reactor is illustrated in Figure 3, where the energy input comprises of biomass flow into the reactor, EGR of hot gases, and water vapor produced during the cooling of the biomass in passage through the cooling screw. Figure 3 also shows where the temperatures of the process are measured. The outgoing energy is comprised of the losses through tubes and reactor, torrefaction gas and the losses of heat through the outgoing biomass.

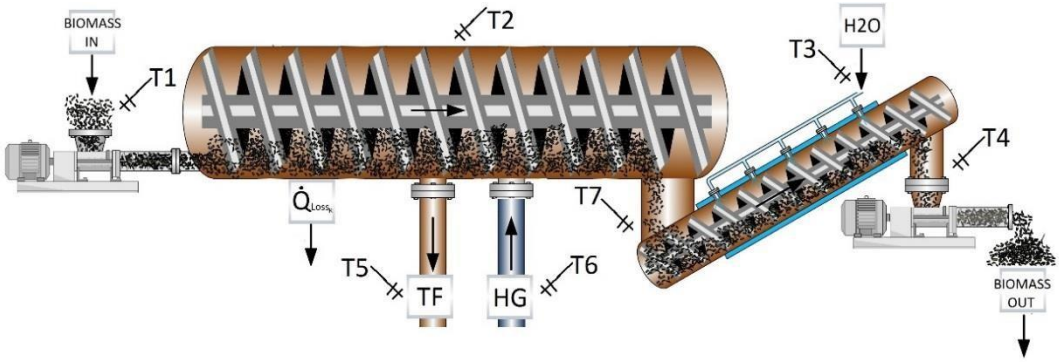

Figure 3 Illustration of the energy flow in the torrefaction reactor

To calculate the effect required by HG to torrefact the biomass flow, data from previous research [19] is used, where a curve fitting was created to determine the needed energy ($\Delta H_{TF\text{Mean}}$) at a variable moisture content (2-10%) of the incoming biomass. The other calculation parameters are reported in Table 2**.**

Table 2 Displays the designing parameters of the reactor; the temperatures can be found in Figure 3. Cp for the torrefied biomass is a mean value calculated from the pilot.

Design Parameters	
MC_{in}	2 - 10%
MC_{out}	0.2%
$T_{gas} = T_7$	375°C
T_1	25°C
T_7	375°C
$C_{P_{Biomass_{out}}}$	1.7kJ/kgK

The effect is then calculated by

$$\dot{Q}_{HG} = \dot{m}_{fin}\Delta H_{TF_{Mean}} \tag{18}$$

To calculate the effect emitted to the system from the biomass at a certain mass yield, the lower heating value (LHV) based on dry substance was determined [19]. Thereafter the effect of the incoming biomass based on LHV was calculated with the following equation.

$$\dot{Q}_{LHV_{in}} = \left(LHV - 2.442\left(\frac{F}{1-F}\right)\right)\frac{\dot{m}_{fin}}{3.6} \tag{19}$$

The higher heating value (HHV) was also determined and provides an input effect of

$$\dot{Q}_{HVV_{in}} = HHV\,\frac{\dot{m}_{fin}}{3.6} \tag{20}$$

to calculate the effect on the output biomass at 74.4% mass yield. Where LHV was determined ($LVH_{74\%}$), the following equation is used

$$\dot{Q}_{LHV_{out}} = LHV_{74\%}\frac{\dot{m}_{fin}}{3.6}0.744 \tag{21}$$

and the effect based on HHV is determined ($HHV_{74\%}$) according to

$$\dot{Q}_{HHV_{out}} = HHV_{74\%}\frac{\dot{m}_{fin}}{3.6}0.744 \tag{22}$$

The heat loss can also be determined when we know the biomass flow out of the reactor, the biomass temperature in and out, and the mean heat capacity displayed in Table 2. This loss is calculated by

$$\dot{Q}_{Loss_{out}} = Cp_{Biomass_{out}}(T_7 - T_1)\dot{m}_{fin}0.744 \tag{23}$$

Losses in the torrefaction reactor and pipelines are calculated with the previously determined loss factor (3%) as

$$\dot{Q}_{Loss_R} = 0.03\dot{Q}_{HG} \tag{24}$$

In order to calculate the effect supplied by steam, we first calculated the required cooling capacity through

$$\dot{Q}_{Cooling} = 0.744\dot{m}_{fin}(T_7 - T_4)Cp_{Biomass_{out}} \quad (25)$$

and then we have to determine a moisture content for the outgoing biomass. The temperature in the biomass when it is leaving the cooling screw and the temperature of incoming water for cooling will also be determined. See these parameters in Table 3.

Table 3 displays the design parameters of the reactor; the temperatures can be found in Figure 3

Reactor Parameters		
MC_{ACS}	12	%
T_3	8	°C
T_4	60	°C
$\lambda_{cooling\ capacity}$	3090	W/m²
A_{shell}	9.4	m²

By equation

$$\dot{m}_{H_2O} = 0.744\dot{m}_{fin}\frac{MC_{ACS}}{(1 - MC_{ACS})} \quad (26)$$

the mass flow of the water required for moistening the torrefied material is calculated. This is then converted to mole flow with the following equation

$$\dot{n}_{H_2O} = \frac{\dot{m}_{H_2O}}{3.6(M_{mol_{H_2}} + \frac{M_{mol_{O_2}}}{2})} \quad (27)$$

and then the enthalpy of water at each temperature can be found in the thermodynamics index [21]. Where the enthalpy is used to find the cooling effect by moistening

$$\dot{Q}_{MC_{ACS}} = \frac{\dot{m}_{H_2O}}{3.6(M_{mol_{H_2}} + \frac{M_{mol_{O_2}}}{2})} \quad (28)$$

The biomass is also cooled by the mantle in the cooling screw that is filled with glycol. This means that the cooling effect on the shell needs to be calculated. We use our readings from the pilot plant to find the cooling capacity of this plant in particular. The cooling capacity of the mantle is calculated through

$$\dot{Q}_{shell} = \lambda_{cp}A_{shell} \quad (29)$$

Then, the effect of the direct water supply used to cool down the biomass to the desired output temperature can be calculated by using

$$\dot{Q}_{H2O} = \dot{Q}_{Cooling} - \dot{Q}_{MC_{ACS}} - \dot{Q}_{shell} \quad (30)$$

To determine the mole flow of water that will evaporate and cool down the biomass to T_4, see Figure 3 The enthalpy of evaporation needs to be found for water at T_3 [21], and then the enthalpy difference between gaseous T_7 and T_3 is added, since the mole flow is determined according to

$$\dot{n}_{cooling} = 3.6\frac{\dot{Q}_{H2O}}{(H_{fgT3} + \Delta H_{T7-T3})} \quad (31)$$

This also means that Q_{H2O} returns to the process, instead of leaving as a loss. This effect is based on HHV (Q_{H2O}=$Q_{H2O_{HHV}}$). We have not subtracted the energy needed for the enthalpy of evaporation. To calculate the Q_{H2O_L}, we use

$$\dot{Q}_{H_2O_{LHV}} = \dot{Q}_{H_2O_{HHV}} - \dot{n}_{cooling} H_{fgT3}(M_{mol_{H_2}} + \frac{M_{mol_{O_2}}}{2}) \quad (32)$$

To go further into the energy and mass balances, we now need to look at the rest of the system; see Figure 4.

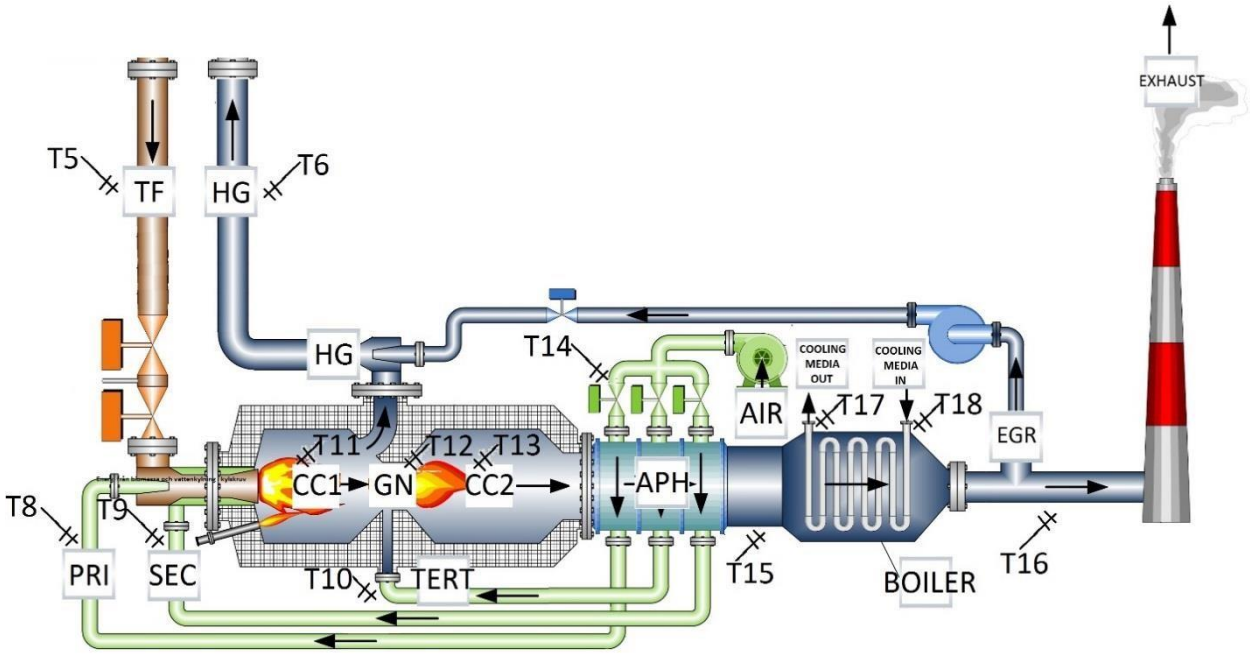

Figure 4 Illustration of the burner process

By locating the system and observing how it is working, we can start the process of finding the air and flue gas compositions. We are interested in determining:

- Flue gas composition in EGR-tube
- Flue gas composition in HG-tube
- Flue gas composition in CC1
- Flue gas composition in GN
- Flue gas composition in CC2
- Air composition in primary air
- Air composition in secondary air
- Air composition in tertiary air
- Air composition in total air.

To determine the percentage of the flue gas recirculated through the EGR, we need to determine the temperature of the hot gas T6. At the IDU, the hot gas reversal is set to 900 ° C, with the result that the dimension of the hot gas tube will be less than if T6 were set to a lower temperature. A drawback of selecting a high temperature is that it mainly leads to the material's ending up in an area known as creep. This means that over a long period of stress, a deformation of the material occurs. Creep deformation is a plastic deformation and has different creep speeds, depending on which phase it is in. The three phases are primary, secondary and tertiary.
If a material enters the creep range, which is heavily dependent on what temperature the material works in and deteriorates in at higher temperatures, the material is in the primary phase, where a rapid deformation occurs, and then slowly goes into the secondary phase. In the tertiary phase, the deformation accelerates until the material breaks. Usually the secondary phase never passes, which the standards are inclined towards. By selecting a low load at high temperature, we could presume that the secondary phase will never be crossed [11].
At the IDU, the maximum pressure of the hot gas tube is selected as 0.5 bar_g. Because of that, Bioendev had to install check valves to make sure that the discharge piping never exceeds this load. Therefore, the dimension of a hot gas exposed to 700 °C will be analyzed, in the hope of passing a higher pressure and, in the best case scenario, avoid the need for check valves and the creep range.
Further, the temperature in the chimney needs to be determined. To avoid condensation, the temperature is set at 180 °C (T16). On the basis of this and knowledge of the hot gas temperature, the enthalpy difference between them can be determined by using the curve fitting of enthalpy as a function of the temperature. The enthalpy difference between the combustion chamber (T11) and the HG piping (T6) can now be determined, noting that T11 is a temperature that will be balanced. Therefore, the calculated value of this is found iteratively, and the first guess is to set the temperature at somewhere around 1100 °C, which is a normal temperature in a burner. We can now calculate the enthalpy difference, between the combustion chamber and the hot gas tube, by using the curve fitting. Then, it becomes possible to calculate the EGR content that goes back into the system by

$$Content_{fg} = \frac{\Delta H_{T11-T6}}{\Delta H_{T6-T16}} \Big/ \left(1 + \frac{\Delta H_{T11-T6}}{\Delta H_{T6-T16}}\right) \tag{33}$$

The mole flow in HG can now be determined, since the temperature of the reactor is set to T7. By using the enthalpy curve fitting and the calculated effect needed (Q_{HG}), we can find the mole flow in HG by using the following equation

$$\dot{n}_{HG} = \frac{\dot{Q}_{HG}}{Content_{fg}\Delta H_{T6-T7} + (1 - Content_{fg})\Delta H_{T6-T7}} \tag{34}$$

Based on this and the ideal gas law, a qualified calculation could be made, to find the dimension that is appropriate for avoiding an excessive pressure drop in the hot gas piping. Because the combustion chamber temperature was assumed to be 1100 °C, we need to check whether this is true. In order to do that, we need to determine the system's other compositions. We already know the flue gas composition in the chimney and the steam generated in the cooling screw. These mole flows are added together as

$$\dot{n}_{H2Otot} = \dot{n}_{H2OChimney} + \dot{n}_{H2OCooling} \tag{35}$$

Based on CC1 at a temperature of 1100 °C, we can now calculate the mole flow and the composition of the EGR, see Table 4.

Table 4 Displays the equation used to determine the flue gas composition in the EGR. (k=fraction, n=mol flow)

Subject	*vol%*	*mol/s*
CO2	$k_{CO_{2EGR}} = \frac{\dot{n}_{EGR_{CO_2}}}{\dot{n}_{EGR}}$	$\dot{n}_{EGR_{CO_2}} = \dot{n}_{HG} Content_{fg} k_{CO_{2Chi}}$
H2O	$k_{H_2O_{EGR}} = \frac{\dot{n}_{EGR_{H_2O}}}{\dot{n}_{EGR}}$	$\dot{n}_{EGR_{H_2O}} = \dot{n}_{HG} Content_{fg} k_{H_2O_{Chi}}$
N2	$k_{N_{2EGR}} = \frac{\dot{n}_{EGR_{N_2}}}{\dot{n}_{EGR}}$	$\dot{n}_{EGR_{N_2}} = \dot{n}_{HG} Content_{fg} k_{N_{2Chi}}$
SO2	$k_{SO_{2EGR}} = \frac{\dot{n}_{EGR_{SO_2}}}{\dot{n}_{EGR}}$	$\dot{n}_{EGR_{SO_2}} = \dot{n}_{HG} Content_{fg} k_{SO_{2Chi}}$
O2	$k_{O_{2EGR}} = \frac{\dot{n}_{EGR_{O_2}}}{\dot{n}_{EGR}}$	$\dot{n}_{EGR_{O_2}} = \dot{n}_{HG} Content_{fg} k_{O_{2Chi}}$
Total	$k_{Total_{EGR}} = k_{CO_{2EGR}} + k_{H_2O_{EGR}} + k_{N_{2EGR}} + k_{SO_{2EGR}} + k_{O_{2EGR}}$	$\dot{n}_{EGR} = \dot{n}_{EGR_{CO_2}} + \dot{n}_{EGR_{H_2O}} + \dot{n}_{EGR_{N_2}} + \dot{n}_{EGR_{SO_2}} + \dot{n}_{EGR_{O_2}}$

Furthermore, we need to determine the flue gas composition of the hot gas in HG. The HG composition is dependent on what the flue gas composition in the CC1 is. And, CC1 depends on the composition in HG because of circulation. Therefore, an iterative calculation is performed, where the first guessed value of HG is assumed to be a bit under the chimney composition. This guess is qualified, because we already calculated the mole flow for the hot gas and for the chimney. This provides a factor that can be used together with knowledge of the composition of the chimney. Then an iteration, between these mole flows and compositions, is started, to find a value that the iteration converges to. This was done with the help of Table 5.

Table 5 Displays the equation used to determine the flue gas composition by iteration in the HG and CC1 there the iterative values are colored red and green.

	Hot gas line		Combustion Chamber 1	
Subject	*vol%*	*mol/s*	*vol%*	*mol/s*
CO2	$k_{CO_2{}_{HG}} = \frac{\dot{n}_{HG\,CO_2}}{\dot{n}_{HG}}$	$\dot{n}_{HG\,CO_2} = \dot{n}_{EGR\,CO_2} + \dot{n}_{HG}(1 - Content_{fg})k_{CO_2{}_{CC1}}$	$k_{CO_2{}_{CC1}} = \frac{\dot{n}_{CC1\,CO_2}}{\dot{n}_{CC1}}$	$\dot{n}_{CC1\,CO_2} = \dot{n}_{HG\,CO_2} + n_{Total\,CO_2}$
H2O	$k_{H_2O_{HG}} = \frac{\dot{n}_{HG\,H_2O}}{\dot{n}_{HG}}$	$\dot{n}_{HG\,H_2O} = \dot{n}_{HG} Content_{fg} k_{H_2O_{CC1}}$	$k_{H_2O_{CC1}} = \frac{\dot{n}_{CC1\,H_2O}}{\dot{n}_{CC1}}$	$\dot{n}_{CC1\,H_2O} = \dot{n}_{HG\,CO_2} + n_{Total\,CO_2}$
N2	$k_{N_2{}_{HG}} = \frac{\dot{n}_{HG\,N_2}}{\dot{n}_{HG}}$	$\dot{n}_{HG\,N_2} = \dot{n}_{HG} Content_{fg} k_{N_2{}_{CC1}}$	$k_{N_2{}_{CC1}} = \frac{\dot{n}_{CC1\,N_2}}{\dot{n}_{CC1}}$	$\dot{n}_{CC1\,N_2} = \dot{n}_{HG\,N_2} + n_{Total\,N_2}$
SO2	$k_{SO_2{}_{HG}} = \frac{\dot{n}_{HG\,SO_2}}{\dot{n}_{HG}}$	$\dot{n}_{HG\,SO_2} = \dot{n}_{HG} Content_{fg} k_{SO_2{}_{CC1}}$	$k_{SO_2{}_{CC1}} = \frac{\dot{n}_{CC1\,SO_2}}{\dot{n}_{CC1}}$	$\dot{n}_{CC1\,SO_2} = \dot{n}_{HG\,SO_2} + n_{Total\,SO_2}$
O2	$k_{O_2{}_{HG}} = \frac{\dot{n}_{HG\,O_2}}{\dot{n}_{HG}}$	$\dot{n}_{HG\,O_2} = \dot{n}_{HG} Content_{fg} k_{O_2{}_{CC1}}$	$k_{O_2{}_{CC1}} = \frac{\dot{n}_{CC1\,O_2}}{\dot{n}_{CC1}}$	$\dot{n}_{CC1\,O_2} = \dot{n}_{HG\,O_2} + n_{Total\,O_2}$
Total	$k_{Total_{HG}} = k_{CO_2{}_{HG}} + k_{H_2O_{HG}} + k_{N_2{}_{HG}} + k_{SO_2{}_{HG}} + k_{O_2{}_{HG}}$	$\dot{n}_{HG}$	$k_{Total_{CC1}} = k_{CO_2{}_{CC1}} + k_{H_2O_{CC1}} + k_{N_2{}_{CC1}} + k_{SO_2{}_{CC1}} + k_{O_2{}_{CC1}}$	$\dot{n}_{CC1} = \dot{n}_{CC1\,CO_2} + \dot{n}_{CC1\,H_2O} + \dot{n}_{CC1\,N_2} + \dot{n}_{CC1\,SO_2} + \dot{n}_{CC1\,O_2}$

Since $Content_{fg}$ was calculated earlier, the composition exiting from CC1 against HG can be determined by using

$$\dot{n}_{SubCH} = \dot{n}_{HG}\left(1 - Content_{fg}\right)k_{SubCC1} \tag{36}$$

where $\dot{n}_{Sub}$ is the mole flow and the index is the subject. k_{SubCC1} is the fraction of the subject in CC1. Thereafter, all mole flow is based on the subject added together to find the total mole flow between CC1 and HG (CH).

Furthermore, the composition in the gas neck (GN) could be determined by subtracting CH from CC1 according to

$$\dot{n}_{SubGN} = \dot{n}_{SubCC1} - \dot{n}_{SubCH} \tag{37}$$

The penultimate flue gas composition is the flow exiting from the chimney just prior to the discharge piping (CHG). It is determined by the previously calculated $Content_{fg}$ and is calculated by using

$$\dot{n}_{SubCHG} = \dot{n}_{HG} Content_{fg} k_{SubChi} \tag{38}$$

To determine the composition of the flue gas in CC2, we need to know the air composition. Therefore, the proportions of the primary and secondary air are set to 50% at lambda 1. This means that lambda 1.3 will set the primary and secondary air to 38.5% each, and the remainder of the air will be sent by the tertiary. The composition of the primary air is determined according to Table 6.

Table 6 displays the equation used to determine the air composition in the primary air.

Subject	*vol%*	*mol/s*
CO2	$k_{CO_{2Prim}} = \frac{\dot{n}_{CO_{2Prim}}}{\dot{n}_{Prim}}$	$\dot{n}_{CO_{2Prim}} = n_{mol_{CO_2}}50\%$
H2O	$k_{H_2O_{Prim}} = \frac{\dot{n}_{H_2O_{Prim}}}{\dot{n}_{Prim}}$	$\dot{n}_{H_2O_{Prim}} = n_{mol_{Fukt}}50\%$
N2	$k_{N_{2Prim}} = \frac{\dot{n}_{N_{2Prim}}}{\dot{n}_{Prim}}$	$\dot{n}_{N_{2Prim}} = (n_{mol_{Ar}} + n_{mol_{N_{2k}}})50\%$
SO2	–	–
O2	$k_{CO_{2Prim}} = \frac{\dot{n}_{O_{2Prim}}}{\dot{n}_{Prim}}$	$\dot{n}_{O_{2Prim}} = O_{2_{Total_{Ds}}}50\%$
Total	$k_{Total_{Prim}} = k_{CO_{2Prim}} + k_{H_2O_{Prim}} + k_{N_{2Prim}} + k_{O_{2Prim}}$	$\dot{n}_{CHG} = \dot{n}_{CO_{2Prim}} + \dot{n}_{H_2O_{Prim}} + \dot{n}_{N_{2Prim}} + \dot{n}_{O_{2Prim}}$

The secondary air is composed in the same manner as the primary. The composition will therefore be determined in the same manner as in Table 6. The tertiary air composition is already calculated in the dry air surplus. Now it is possible to calculate the flue gas composition in CC2. This is done by

$$\dot{n}_{SubCC2} = \dot{n}_{SubCC1} - \dot{n}_{SubCH} + \dot{n}_{SubTert} \quad (39)$$

We can now begin calculating energy balance, where the temperature after the air preheater (APH) controls how much energy should go off to the glycol loop in the boiler. By determining the temperature of this, we can analyse the temperature needed to balance the energy of the CC1.
As earlier mentioned, the flue gases leaving the chimney are set to 180° C, to avoid condensation problems. Therefore, it is possible to determine the effect of what leaves the chimney at 25°C, because we have also calculated the mole flow that is departing. We do this with the following equation

$$\dot{Q}_{Chimney_{LHV}} = \dot{n}_{Chi}\Delta H_{T16-Tair} \quad (40)$$

Since we have guessed the temperature after APH, this allows calculation and adjustment of the effect that will shift to the glycol loop in the boiler by varying T15. The effect departing is given by

$$\dot{Q}_{Boiler} = \dot{n}_{CC2}\Delta H_{T15-T16} \quad (41)$$

The energy balance is complete when the sum of all these effects becomes zero by means of varying T15.
When the temperatures are finally set, the mole flow through the hot gas pipe can be determined. By varying the tube diameter, the velocity can be adjusted to 20 m/s to avoid high pressure drop in the tube. By using an Excel document as described in the theory section, the size of the pipe that leads the hot gas can now be designed. By changing the moisture content between 3 and 10%, temperatures between 700 and 900° C and balancing the system, in the different cases at ten different NPC, we produced a chart for designing the right pipe dimension at a specific case.

2.2 Dimensioning bursting disc

The main reason that NFPA 68: 2007 was used, instead of EN 14491: 2006, is that EN 14491: 2006 does not apply to P_{red} higher than 2 bar_g. P_{red} is the reduced maximum pressure of the explosion after the bursting disc has broken.
The calculations are according to EN14491: 2006, where P_{red} was set to 2 bar_g and P_{stat} to 0.14 bar_g. P_{stat} is the static opening pressure of the bursting disc. This provides negative results for the selected application, which showed great difficulties in producing a bursting disc that can handle 500 °C with such a low opening pressure as 0.14 bar_g.
In addition, the design of the bursting disc needs to be for a spread of 10%, perhaps even as much as 30% of the opening pressure. This means there is an opening pressure between 0.1 to 0.14 bar_g, since the pressure cannot exceed 50% of P_{stat} in normal operation. This means that one of the selected bursting discs should not exceed 50 $mbar_g$, which in the current application must be considered very low. This implies a great risk of leading to ruptured bursting discs in leakage tests.
Note that the containment of the reactor, cooling screw, extruder screw at calculations and simulations according to PED, handles 9 bar_g at 20 °C, as the number of cycles are less than 200 cycles/year. At 500 °C, the same components can handle 3.5 bar_g. On the other hand, these are not designed for a dust explosion, but for a gas explosion, which, according to previous calculations, gives a P_{max} of 2.4 bar_g. This is mainly due to the severe limitation of free oxygen, because the formed pyrolysis gas creates an overpressure that keeps away incoming air. The reason that 9 bar_g is not used in the calculations is because we have other components of the reactor that are not rated for 9 bar_g, such as screws, plugs and oxygen sensors. To calculate the ventilation area, NFPA 68: 2007 is used, according to Chapter 8, as shown in Figure 5 below.

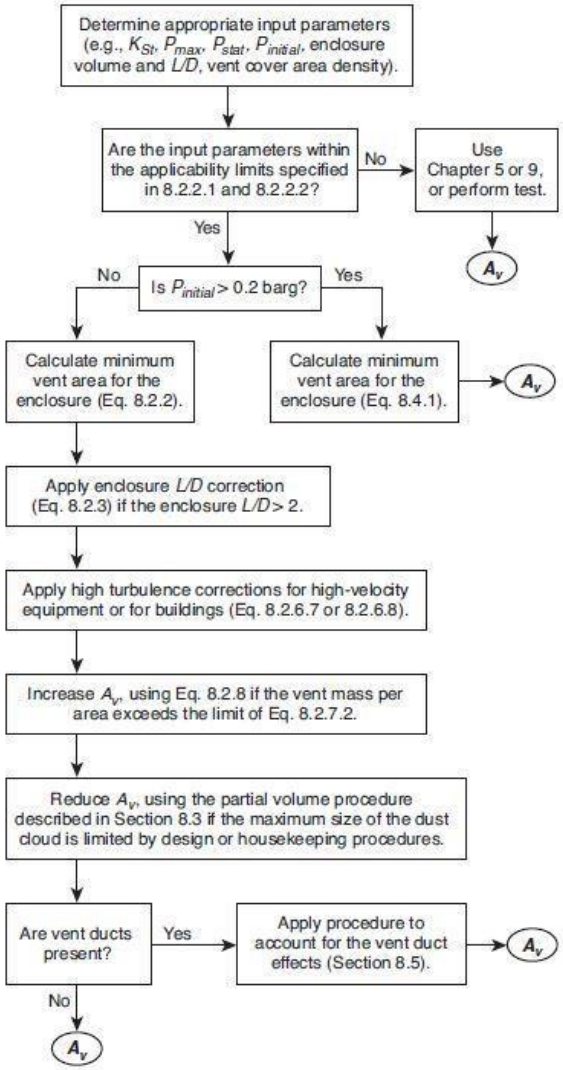

Figure 5 Dust Explosion Vent Sizing Calculation Flowchart for Chapter 8, NFPA 68:2007.

The last step in designing the bursting discs consisted of carrying out a situation analysis. The following operating parameters shown in Table 7 were sent to the vendors used for this project.

Table 7 displays the designing parameters of the bursting discs

Bursting discs parameters		
Pmax	8.7	*barg*
Pstat	0.5	*barg*
Pred	4.5	*barg*
Tmax	500	*°C*

To prevent the air inside the reactor from condensing against the bursting discs, the bursting discs need to withstand the heat that the electricity tracing is producing to avoid cold surfaces. After the market analysis was done, it was found that a vendor in England could develop and manufacture a rupture disk that passed these requirements in DN750. By knowing the area of the bursting disc, the number of bursting discs and the dimensions of the pipes could be determined.

At this stage, it was also interesting to examine and calculate what area the ventilation needed to be if P_{red} were to be reduced to $2bar_g$. This could entail a minor cost, since the steel in the reactor can be thinner than if P_{red} is set to $4.5bar_g$.

2.3 Dimensioning of check valves/pressure reducer

At the IDU, Bioendev uses check valves to protect the hot gas tubing from high pressures if an explosion occurs. To investigate how quickly the check valve icloses, Bioendev AB uses Autodesk CFD 2016 to simulate and analyze the shutter speed. To avoid singularities and errors in the simulation, several simulations have been performed, where the mesh was refined until the results converged. In a scaling-up of the IDU, the diameter of the hot gas tube will increase, in accordance with the design that was shown in previous chapters.
Therefore, a new check valve was constructed in the appropriate size. Thereafter, a new analysis was performed by using simulations to investigate whether pressure wave propagation is reduced enough, to make sure that the hot gas tubing will not burst in an explosion.
As a supplement to the report, a further investigation is proposed. In case the results prove that the temperature of the hot gas must withstand 900°C, and the check valves physically turn out to be too large, a design study of a new idea to solve these difficulties was performed. The idea was to use baffles in the form of cones, where the baffle system allows a hot-gas flow to pass through with a minimal pressure drop in one direction. If an explosion with a blast in the opposite direction were to occur, the blast would reduce itself by creating a large pressure drop. In this thesis, this idea is named BPS (baffle for pressure surge), which is inspired by flash suppressors, which have the task of reducing the recoil when firing a weapon.
To begin the analysis of the check valves, the first thing was to find the shutter speed for the existing check valves, to compare with larger valves; see Figure 6**.**

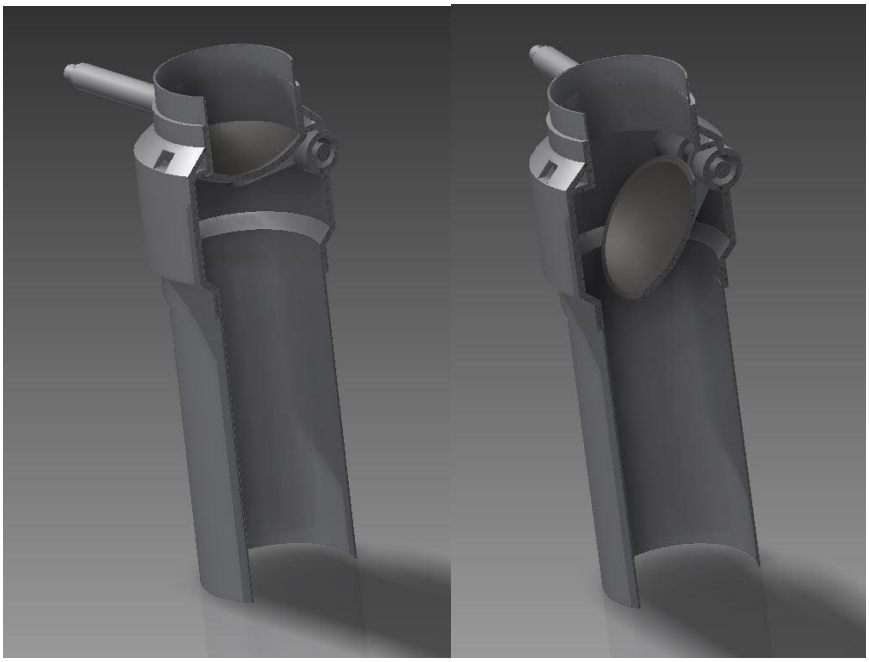

Figure 6 Illustration of a closed and an open valve.

Then the static pressure was analyzed in the system to check that P_{max} did not exceed $0.5bar_g$; see Figure 7.

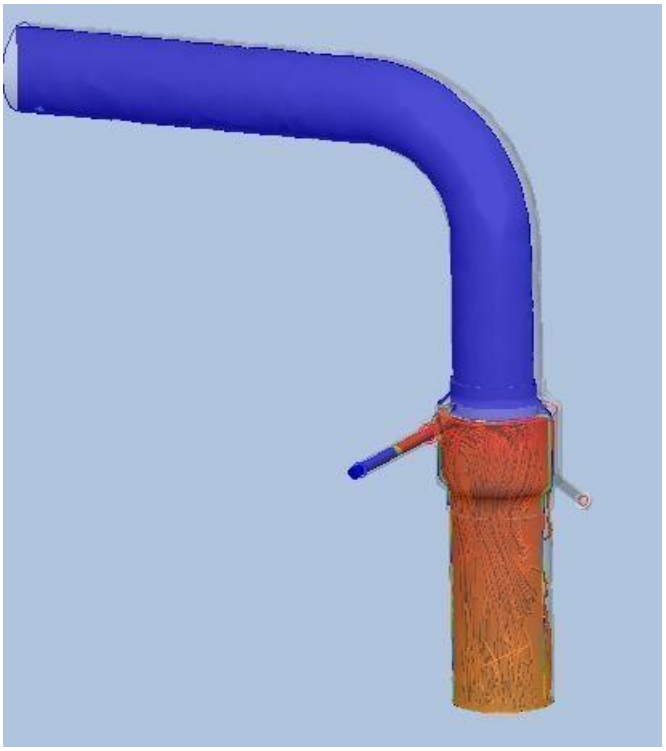

Figure 7 Show how the check valve reduced the pressure, just after the valve is closed.

Figure 7 shows the static pressure in a range of colors, where the blue is under 0.5bar$_g$ and red shows the maximum pressure that occurs. Since the maximum pressure was obtained in this study, it was possible to design the check valve to manage these pressures. The results then iteratively moved back and forth between the FEM and CFD until a satisfactory result was achieved. After that, a check valve with much greater area was designed in a similar way to determine if the valve cover and the weight actuated the safety.

In a similar way, a model with baffles was constructed see Figure 8. The main difference between this and a flash suppressor is that the BPS must be analyzed in both directions. This is because the hot-gas flow under normal conditions goes through the BPS in the opposite direction than the blast from the explosion.

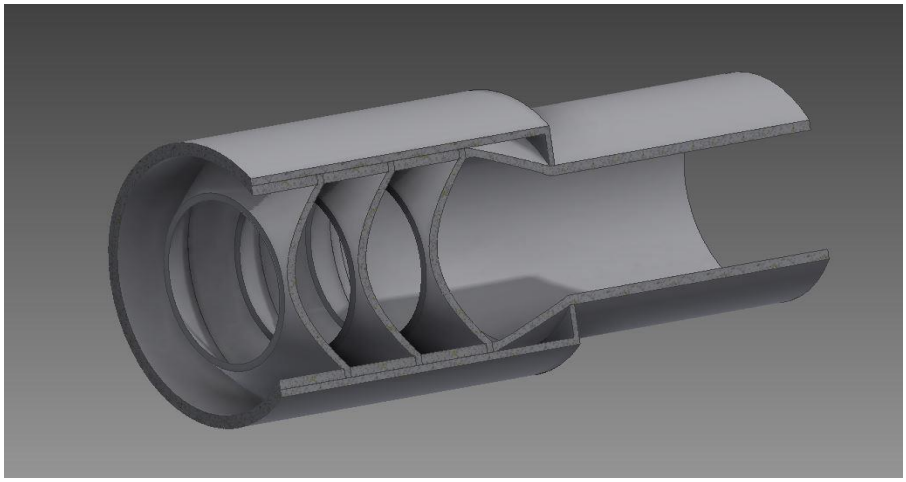

Figure 8 Illustration of the final design of the BPS.

Figure 8 shows the study's best design, according to the conclusions. In order to obtain a low-pressure drop in operating conditions, the inner diameter of the cone must be at least as large as the hot gas tube diameter. This solution stops the pressure wave efficiently, without moving parts; see Figure 9.

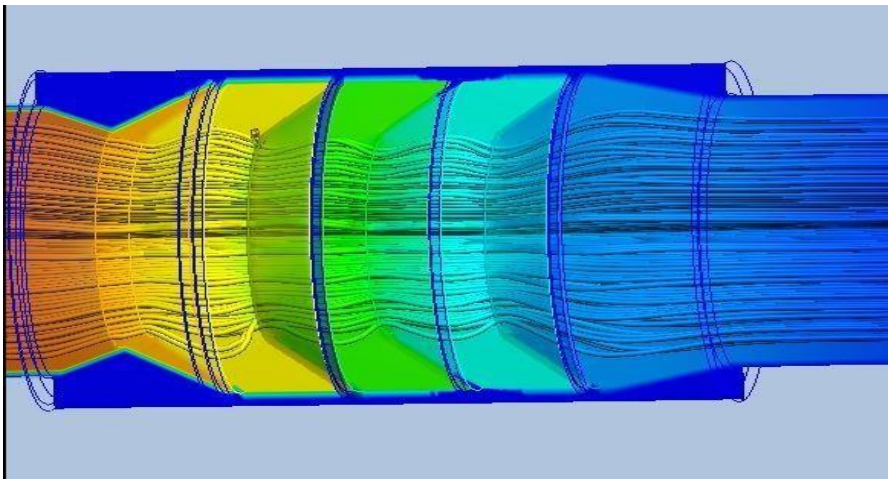

Figure 9 CFD simulation of a pressure reduction in the BPS at an explosion at 4,5barg.

To find a durable construction, the BPS needed to be iterated between CFD and FEM. In Figure 10, a BPS with an inner diameter of DN800 is simulated and withstands an explosion pressure at 4.5bar$_g$ and also reduces it to under 0.5bar$_g$. The total length of the BPS module was 1600mm.

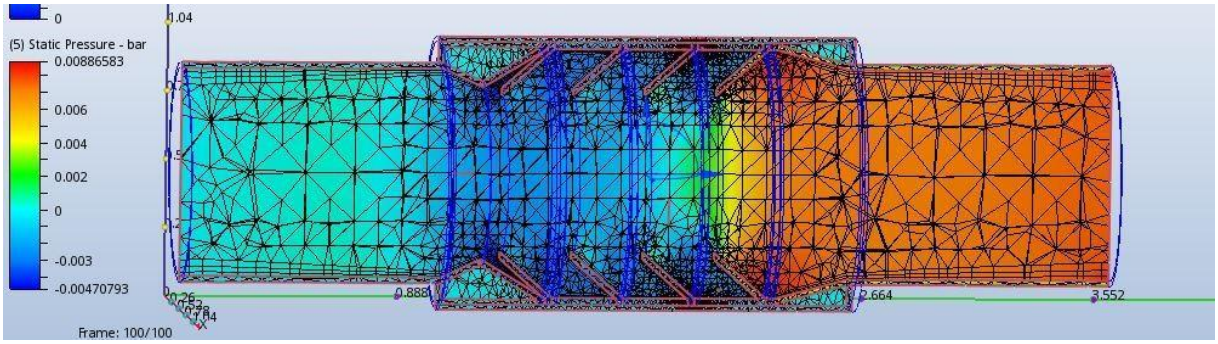

Figure 10 CFD simulation of static pressure drop, at normal operating flow, 20m/s.

After the explosion simulation, the operation flow was simulated, in the opposite direction at 20 m/s. The simulation shows that the pressure drop is not very high; the design can of course be improved. When these simulations were finally performed, it was interesting to set the BPS against the check valve. Therefore, a new valve, size DN 800, was designed.

3. Methods

3.1 Identifying components and system structure

To identify the vital components of the torrefaction system and operational parameters, it was important to be able to determine flows and how these operate inside the system. In this step, it was also important to determine the vital temperatures, such as flue gas exiting the chimney and the hot gas tube operating temperature, in the system. In this subsection, the standards were studied, including steel products and their properties.

3.2 Energy and mass balance

Since the structure of the system was known, it was possible to begin the calculations of the energy and mass balances in the system.

3.2.1 Fuel calculation

The biomass data in this study was from an available elementary analysis, and heating value analyses were used [19].

By using the heating value and the mass yield through the system, one could see how much gas developed per kilogram of dry biomass, as well as the composition of the gas. Then, calculation of combustion could begin. By determining the moisture content of the biomass when it enters the torrefaction process from the drying system, it is possible to determine how many moles of water discharge from the biomass to the flue gases. According to this, the mass of the total fuel gas can be determined, as can the total oxygen demand per kg of dry biomass.

In order to proceed further and determine the total stoichiometric air requirements that will be needed in the burning process, one needs to determine the raw nitrogen that enters into the combustion with the air, because it is not actively involved in the combustion. The molar amount of dry air that is crucial for the combustion can be calculated by adding the oxygen of the dry air to the molar amount of the raw nitrogen.

In addition to the air composition, there is also moisture in the air that does not bind molecularly. This moisture is assumed to be 1% of the dry air. With these assumptions and data, the stoichiometric air requirement for combustion can be calculated for each kg of dry substance biomass.

After the stoichiometric combustion gases have been determined, we need to set an excess air. Lambda needs to be greater than 1; in this calculation, lambda is determined to be 1.3. The dry air, the moisture and the dry flue gases can then be determined.

3.2.2 Flue gas calculation

Flue gas calculation will need to be done to determine the theoretical emission values, and how the flue gas will transport heat through the system as well as how the flue gas will expand in the different parts of the system, in accordance with temperature changes. This makes it possible to determine mole flow of gases through the chimney, and its composition, based on the biomass flow into the reactor, noting that the molar mass in and out of the system is different. It will increase in the combustion. This can be attributed mostly to the combustion of the hydrogen from the fuel and the fact that the fuel has to contain moisture to evaporate.

Even the steam generated in the cooling screw needs to be calculated. Since the mole flow in the chimney has been determined, we know what is coming into and what is coming out of the system. In the literature review, a full approach for these calculations was studied and a template based on this was used in Excel [22].

3.3 Reactor Design

The reactor was designed according to demands that were found in the standards for pressure vessels. It was also designed on the basis of a physical limitation found through tests on the reactor at the IDU, where the degree of filling was found to be the main limitation of the volume of biomass through the reactor.

3.4 Dimensioning bursting disc

To calculate the ventilation area needed to reduce the pressure of an explosion, NFPA 68: 2007 was followed.

3.5 Simulations

Simulations of flows were made primarily to study the pressure drop across the components in the system. Even simulations with moving parts were performed, to study the shutter speed at higher pressure shocks. In this step, the literature on dust explosion and its distribution was studied. The simulations were performed with the computer program, Autodesk CFD 2016. In all simulations, Nodal Aspect Ratio (NAR) was used. A value of NAR < 100 is ideal in regions of interest. This is the max-to-min ratio of all element edge-lengths emanating from a mesh node and can be regarded as a measure of the distortion of an element. The fluid mechanical equations are then applied to the mesh and are solved by an iterative process. The results of each iteration will be slightly different from the previous one. In a successful simulation, the changes will become increasingly smaller, to a point where the iterations will not add any new information to the outcomes. When this happens, the simulation is said to have converged. For boundary conditions, the inflow was set to 20 m/s at the investigation of the pressure drop in normal conditions. The outflow condition was set as a gage pressure of 0 (free outflow), and the top and side boundary conditions were set to slip/symmetry. The k-ε turbulence model was used. For the explosion simulation, the outflow condition was set as a gage pressure of 4.5 $bar_{g,}$ and the opposite 0 bar_{g}. In further investigations, a small real model of the BPS should be made to verify the results from the simulations.

3.6 The Finite Element Method

Through the literature review, properties such as yield strength and creep range were obtained for different steel materials. With this knowledge, an F.E.A was done on the object to see if it would hold or brake from a pressure shock. In this operation, it is also important to know the operating temperatures. Since the system has very high temperatures, material often ends up in the creep range. This means that a component can withstand a pressure shock, but can rupture over time. F.E.M were performed with the computer program Autodesk Inventor 2016. To investigate the forces that prevail over time at the flanges, the whole tubing system has to be drawn and specified. This was not done in this study.

4 Results and Discussion

4.1 Reactor design

The design of the new reactor is obtained by the geometric formula, where the volume was the limiting factor. Construction of a facility 10 times larger than the existing one implies very large risks, since elements that in a smaller facility have no significance can be the cause of malfunction in a larger facility.

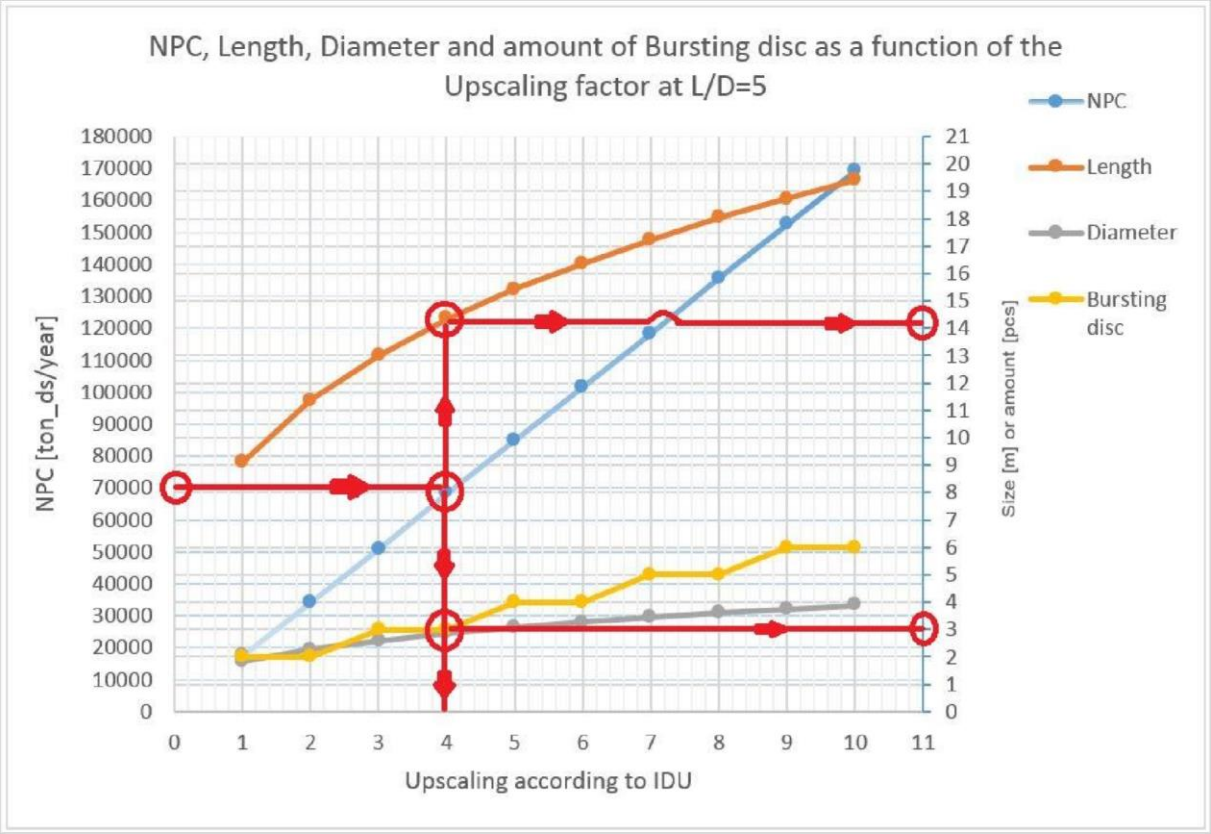

Figure 11 displays the reactor design according to NPC or Upscaling from IDU. The amount of bursting discs in size DN750 are also displayed. The red path show an example how to read the diagram. NPC = 70 000tonDS/y, Length =14.2m, Bursting disc = 3pcs, Diameter = 3m, Upscaling factor according to IDU = 4.

According to Figure 11 the reactor needs to be 19,5m long and 4m in diameter, at 10 times greater capacity. According to NFPA 68: 2007, the reactor needs 6 pcs of bursting discs. If the reactors P_{red} were set to $2bar_g$, 14pcs of bursting discs in DN 750 would be required. This means that the installation space, with insulation included, will be too small, and there will be no room for the torrefaction gas pipe, nor for the hot gas pipe. Therefore, P_{red} must be set to $4.5bar_g$.

In terms of shipping problems, the size of the reactor should not pose any major difficulties to transport. When shipping a larger facility, it may be necessary to weld connecting pieces and sections on site after delivery.

A matter that has not been raised in this thesis is the feeding screw in the reactor. A study should be done to see what will happen to the feeding screw upon upscaling, because there are large temperature differences prevailing in the reactor from the cold biomass feed to the hot outgoing material.

4.2 Design of hot gas tube reversal

The results of dimensioning the hot gas tube can be seen in Figure 12. The results are based on a constant flow rate in the tube for all sizes. The velocity is set to 20m/s.

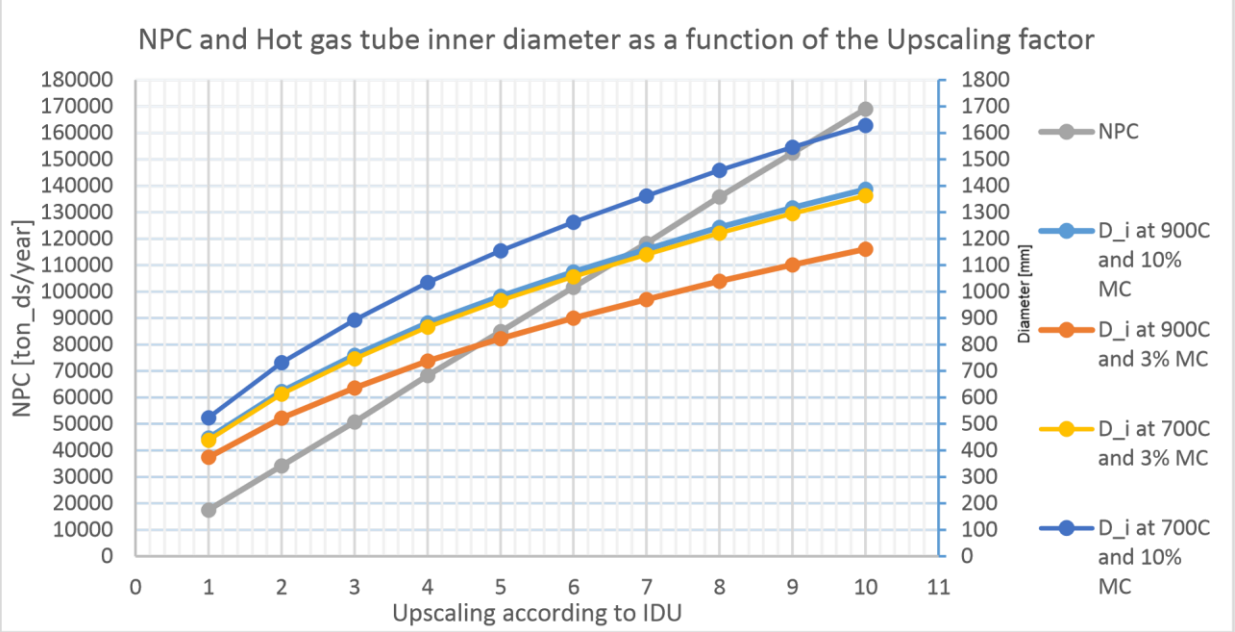

Figure 12 displays the inner diameter of the hot gas tube according to design temperature and moisture. The diagram is read in same manner as in Figure 11

The graph in Figure 12 shows the inner diameter of the hot gas main tube. The graph also shows how great the differences in effect on the pipe diameter are, between the operating temperature of the hot gas and the moisture content of the incoming material.

We can also see that a system needs different pipe sizes, depending on humidity and temperature. For example, we can use the same pipe diameter for an NPC at 170000 ton_{DS}/y_{out}, when the moisture content is 10% and the hot gas tube is designed to withstand 900° C, as when the moisture content was 3% and the hot gas tube was designed for 700° C.

The problem with a hot gas line designed for 700° C and 3% moisture is that if the incoming moisture content increases to 10%, the pipe diameter needs to increase from DN1400 to DN1650 to meet the energy demand for torrefaction of biomass to a mass yield of 75%. The advantage of having a tube that is designed for an operating temperature of 700° C is that the pipe can withstand higher loads. We must also take into consideration that the steel used (253MA) at 900° C is a variant of 4828, which has an increased nitrogen content and has been micro-alloyed with rare earth metals (REM). The most suitable temperature range is 850-1100° C, because structural changes, when used between 600 and 850° C, can lead to reduced impact toughness at room temperature. Therefore, Inconel 625 can be recommended, because of its high allowable design strength at elevated temperatures, especially between 649-760° C [23] [24].

Therefore, a comparison should be carried out. It should compare the extra cost of installing a larger dimension of the pipe, but which results in eliminating the need to install check valves, with the cost of installing a smaller dimension, but in which the cost of the check valves must be added.

It is worth mentioning that it will still be necessary to install valves to control the pressure and flow into the reactor. This is an additional cost that needs to be added to the design of a 700° C pipe. But, given that the hot gas check valves need to be designed and custom-made, it might be economically advantageous to use a larger pipe size anyway.

We also see that the dimensions of the components flatten out, while the NPC increases linearly. Therefore, if considering only capital expenses, it is economical to build large plants.

3.3 BPS

During the simulation of the BPS, an analysis was performed to study the flow through the BPS during normal conditions.

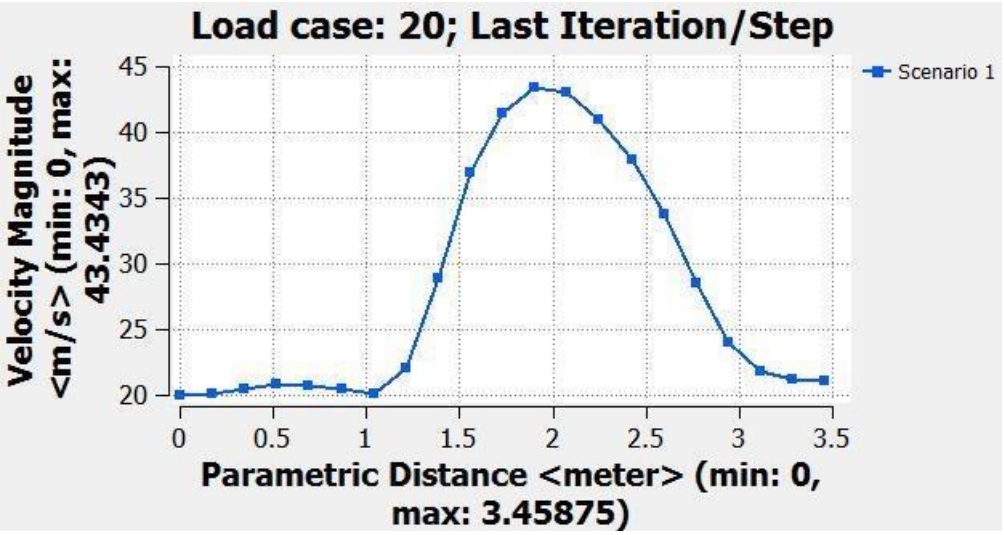

Figure 13 Velocity through the BPS.

Figure 13 shows that the maximum speed through the BPS was 44m/s. The flow went into the BPS after 980mm and out after 2570mm (BPS measures 1590). As we see, in Figure 14**,** the velocity goes down to a normal level about 600mm after leaving the BPS. This is good, because a high inlet velocity into the reactor will affect the center axis of the feeding screw, with a high risk of incurring heat-related problems.

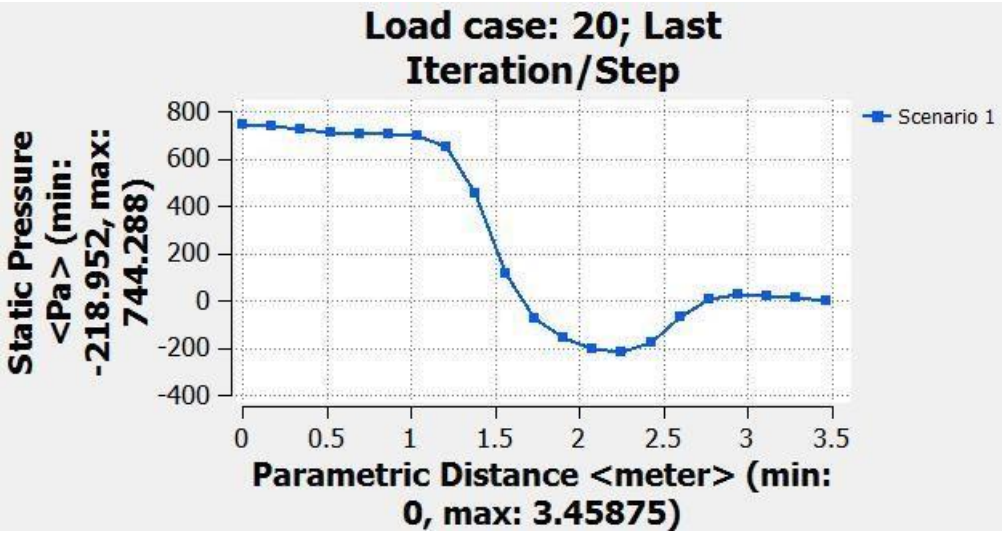

Figure 14 Pressure drop through BPS in normal use.

In Figure 14 we see that the pressure drop through the BPS is about 300 Pa/m compared to 100 Pa/m, which is usually designed for ventilation systems; this drop could be considered to be acceptable.

4.4 Check valve

Figure 15**,** below, shows that the pressure drop in the normal direction of the check valve is about 350 Pa/m.

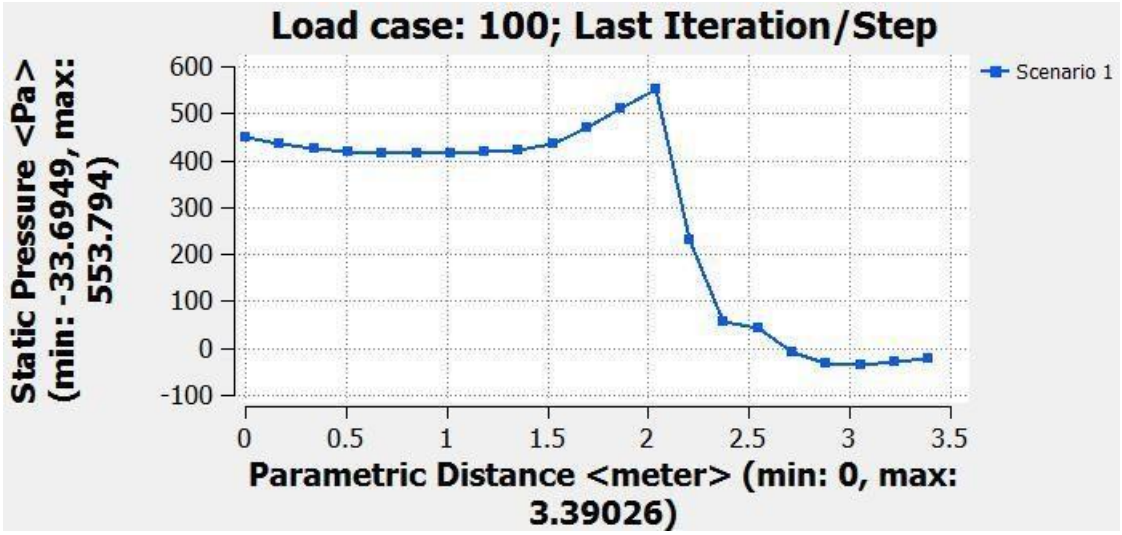

Figure 15 Pressure drop through the check valve in normal use.

The shutter speed of a check valve with DN850 was analyzed, where we could assume that the time would increase, because the force on the valve cap increases with the area, and the mass of the valve cover increases in line with the volume. The difference was still relatively low where the shutter speed was 0,093 seconds, compared with the check valve DN300, which closed at 0,076 seconds. This test was done merely by scaling up the valve geometric. Therefore, a quick FEA was done to see if the check valve was resistant to an explosion; see Figure 16.

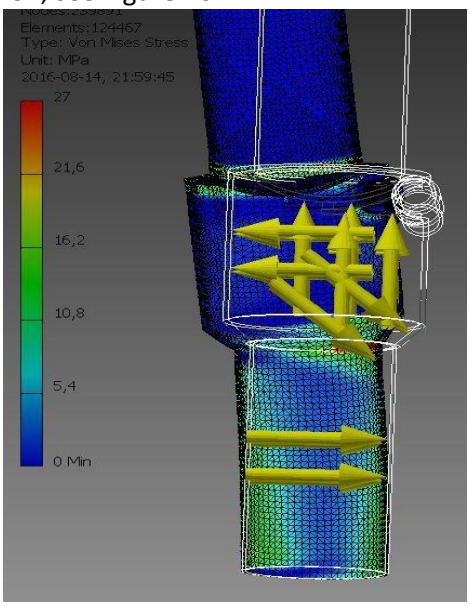

Figure 16 displays the Von Mises Stress in the FEM analyze on the check valve in DN850.

In Figure 16, it was found by studying the rupture strength that the check valve managed an explosion. The lifetime can be set extremely low, since an explosion takes place very quickly and not continuously. Therefore, the flange load will become the design limit, as these are constantly subjected to a load and the temperature makes them work into the creep range. In order to implement these loads in an FEA, the entire piping system with hanger must be drawn and analyzed to find the loads exposed to the flange.

5 Conclusions

In order to take a final decision about what size the IDU can be scaled to, the conveyor screw needs to be investigated, regarding how big it could be, depending on self-weight ratio, heat, and especially the design.
In this thesis, the sizing was made by scaling the system geometrically, based on benchmark tests on the IDU. This only provides a hint of the right solution. This report therefore provides qualified design measures for a further investigation of the construction.

One of the technical challenges was to investigate the check valve and what problems a bigger system might be exposed to, and how that will affect the function of the check valve. In my study, there was no sign that the check valve, nor the BPS, will be a problem. An analysis with an economic aspect should be performed, to investigate whether one of these is preferable. Mechanically, the BPS is preferable, since it is without moving parts.

There was also an investigation of whether the reactor should be designed for a lower pressure. The results showed that there was not enough external space around the reactor for the required amount of bursting discs.

6 References

[1] H. Gefwert, ”Klimatmötet COP21 i Paris,” Regeringen, Regeringskansliet, 12 12 2015. [Online]. Available: http://www.regeringen.se/sveriges-regering/miljo--och-energidepartementet/klimatmotet-cop21-i-paris/.

[2] N. Skoglund, ”Ash chemistry and fuel design focusing on combustion of phosphorus-risch biomassm,” Umeå, 2014.

[3] European Parliament and of the Council, ”EUR-Lex,” 23 04 2009. [Online]. Available: http://eur-lex.europa.eu/legal-content/EN/ALL/?uri=CELEX:32009L0028.

[4] European Parliament and of the Council, ”EUR-Lex,” 23 10 2001. [Online]. Available: http://eur-lex.europa.eu/legal-content/EN/TXT/?uri=CELEX:32001L0080.

[5] H. P och J. P, ”Regulation of Energy from Solid Biomass Plants,” 2006.

[6] Svebio, ”Svebio,” 2015. [Online]. Available: https://www.svebio.se/om-bioenergi/biovarme/.

[7] K.-G. Lindblad, ”Kolning,” 1998. [Online]. Available: http://www.forntidateknik.z.se/IFT/litte/littekgl/kolkgl.htm. [Använd 12 12 2015].

[8] R. Zanzi Vigouroux, ”Pyrolysis of biomass,” Stockholm, 2001.

[9] P. A. Brownsort, ”Biomass pyrolysis process,” 2009.

[10] A. Bates, The Biochar Solution, New Society Publishers, 2010, pp. 93-120.

[11] J. Lehmann and S. Joseph, Biochar for Environmental Management., vol. Second edition, 2009, p. Chapter 3.

[12] H. P. Schmidt, S. Abiven, C. Kammann, B. Glaser, T. Bucheli och J. Leifeld, ”Guidelines,” European Biochar Foundation , 2016.

[13] Erik Dahlquist, Technologies for Converting Biomass to Useful Energy, Taylor & Francis Group, 2013, pp. 218-229.

[14] Utbildningsstyrelsen, ”Laboratorieanalyser,” 2012. [Online]. Available: http://www.edu.fi/extraktivamnen_i_cellulosamassa. [Använd 12 12 2015].

[15] Bioendev AB, ”Bioendev,” 2016. [Online]. Available: www.bioendev.se.

[16] D. Bjerketvedt, J. R. Bakke och K. v. Wingerden, ”GEXCON,” 24 12 2012. [Online]. Available: http://www.gexcon.com/article/handbook-chapter-1#sect1_1.

[17] J. García-Torrent, E. Conde-Lázaro, C. Wilén och A. Rautalin, Fuel, vol. 77, Elsevier Ltd, 1998.

[18] R. Zalosh, ”Dust Explosion Fundamentals,” 2011.

[19] M. J. Prins, ”Thermodynamic analysis of biomass gasification and torrefaction,” Technische Universiteit Eindhoven, 2005.

[20] Y. A. Cengel och M. A. Boles, Thermodynamics, Mcgraw-hill Education, 2007.

[21] L. Wester, ”Kurspärm,” i *Förbränning och Rökgasrening*, Västerås, Umeå Universitet, 2013.

[22] Harald Pihl AB, ”Harald Pihl,” [Online]. Available: http://www.haraldpihl.se/.

[23] A. Edrisi, ”Riskmodell för utökat underhållsintervall på ångturbiner,” 2013.

[24] I. Barin, Thermochemical Data of Pure Substances, 2008.